An Improvement of Roughness Height Parameterization of the Surface Energy Balance System (SEBS) over the Tibetan Plateau

XUELONG CHEN

Key Laboratory of Tibetan Environment Changes and Land Surface Processes, Institute of Tibetan Plateau Research, Chinese Academy of Sciences, Beijing, China, and Faculty of Geo-Information Science and Earth Observation, University of Twente, Enschede, Netherlands

ZHONGBO SU

Faculty of Geo-Information Science and Earth Observation, University of Twente, Enschede, Netherlands

YAOMING MA AND KUN YANG

Key Laboratory of Tibetan Environment Changes and Land Surface Processes, Institute of Tibetan Plateau Research, Chinese Academy of Sciences, Beijing, China

JUN WEN AND YU ZHANG

Key Laboratory of Land Surface Process and Climate Change in Cold and Arid Regions, Cold and Arid Regions Environmental and Engineering Research Institute, Chinese Academy of Sciences, Lanzhou, Gansu, China

(Manuscript received 21 February 2012, in final form 28 August 2012)

ABSTRACT

Roughness height for heat transfer is a crucial parameter in the estimation of sensible heat flux. In this study, the performance of the Surface Energy Balance System (SEBS) has been tested and evaluated for typical land surfaces on the Tibetan Plateau on the basis of time series of observations at four sites with bare soil, sparse canopy, dense canopy, and snow surface, respectively. Both under- and overestimation at low and high sensible heat fluxes by SEBS was discovered. Through sensitivity analyses, it was identified that these biases are related to the SEBS parameterization of bare soil's excess resistance to heat transfer (kB^{-1}, where k is the von Kármán constant and B^{-1} is the Stanton number). The kB^{-1} of bare soil in SEBS was replaced. The results show that the revised model performs better than the original model.

1. Introduction

Because of the elevation of the Tibetan Plateau, energy and water are exchanged between the surface and the middle troposphere above it. The growing interest in the interaction between atmosphere and plateau surface is driven by the realization that the thermal effects of the plateau may influence atmospheric circulation in the Northern Hemisphere (Tao and Ding 1981; Wang et al. 2011). The lack of observational datasets on the interactions between the whole plateau and the atmosphere above makes it difficult for us to quantitatively analyze the variation in energy and water exchanges in this region.

Conventional meteorological techniques that employ point measurements to estimate the components of the surface energy balance represent work on a local scale (Su et al. 2006). Remote sensing enables us to estimate surface fluxes from local to regional scales and offers the possibility to derive the regional distribution of land surface heat fluxes over little-instrumented and sparsely populated areas. Recent studies have explored remote sensing approaches to estimate the regional distribution of surface heat fluxes (Ma et al. 2003, 2008b, 2011). The Surface Energy Balance System (SEBS) developed by Su (2002) can estimate turbulent heat fluxes

Corresponding author address: Xuelong Chen, Faculty of Geo-Information Science and Earth Observation, Water Resources Dept., University of Twente, Hengelostraat 99, 7514 AE Enschede, Netherlands.
E-mail: chen24746@itc.nl

DOI: 10.1175/JAMC-D-12-056.1

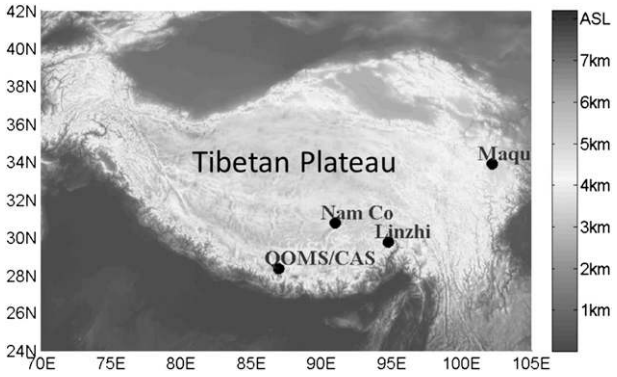

FIG. 1. Positioning of the QOMS/CAS, Nam Co, Linzhi, and Maqu stations on the Tibetan Plateau.

from point to continental scale with reasonable accuracy using satellite and meteorological data (Su et al. 2005; Oku et al. 2007, etc.). Although significant progress has been made, further efforts are needed to improve the accuracy of SEBS over the Tibetan Plateau regions (Su et al. 2006).

The roughness height for heat transfer z_{0h} needs to be determined to accurately calculate the sensible heat flux by means of the Monin–Obukhov similarity theory (MOST) and SEBS:

$$H = ku_*\rho C_p(\theta_0 - \theta_a) \times \left[\ln\left(\frac{z-d}{z_{0h}}\right) - \Psi_h\left(\frac{z-d}{L}\right) + \Psi_h\left(\frac{z_{0h}}{L}\right)\right]^{-1}, \quad (1)$$

where z is the height above the surface, u_* is the friction velocity, ρ is the density of air, C_p is the specific heat for moist air, k is the von Kármán constant, d is the zero plane displacement height, θ_0 is the potential temperature at the surface, θ_a is the potential air temperature at height z, H is the sensible heat flux, Ψ_h is the stability correction functions for sensible heat transfer, and L is the Obukhov length.

The scalar roughness height for heat transfer can be derived from

$$z_{0h} = z_{0m}/\exp(kB^{-1}), \quad (2)$$

where z_{0m} is the roughness height for momentum transfer and kB^{-1} is the excess resistance for heat transportation, with k again being the von Kármán constant and B^{-1} being the Stanton number. The quantity kB^{-1} has been the subject of much study (Sheppard 1958; Owen and Thomson 1963; Brutsaert 1982; Beljaars and Holtslag 1991; Zeng and Dickinson 1998; Su et al. 2001; Kanda et al. 2007). Few formulas are able to describe the observed diurnal variation in kB^{-1} over the Tibetan Plateau (Ma et al. 2009). A kB^{-1} scheme that can account for the diurnal variations in thermal roughness length performs best in turbulent heat flux estimations and land surface modeling (Yang et al. 2008; Chen et al. 2011).

SEBS has been widely used to estimate the surface energy balance and evapotranspiration in different areas; further analysis of the uncertainties has been limited, however. Surface heat fluxes depend on many parameters, such as vegetation, soil type, soil moisture, and snow cover. Sensitivity analysis can assist in the identification of the most sensitive parameters for quantifying model uncertainty and consequently can provide valuable insight into the degree of effort that should be expended to constrain errors in a model. The sensitivity of sensible heat flux estimates from SEBS has not yet been fully examined.

In this study, we first tested at four different land cover units whether SEBS driven by boundary layer meteorological measurements, as opposed to tower-based flux measurements, can be used to derive items of surface energy balance over the Tibetan Plateau. Then, we evaluated the impact of varying parameters on H estimates from SEBS and used this information to try to identify the causes of SEBS's biases. Sensitivity analysis of SEBS is conducted by comparing the output of varying input parameters with eddy covariance. A year of meteorological data and ancillary parameters were compiled at four sites to perform a sensitivity analysis of SEBS. We then improved the turbulent heat parameterization in SEBS—to be specific, the equation for kB^{-1}.

In section 2, we present the instrumentations, data processing, and points evaluations as well as discuss the problem of kB^{-1} in SEBS. A sensitivity-analysis method and the results are included in section 3. The discussion and conclusions are presented in section 4.

2. Problem analysis

a. Data

Data used in this paper were collected at four research stations on the Tibetan Plateau: Qomolangma Station for Atmospheric and Environmental Observation and Research from the Chinese Academy of Sciences (hereinafter QOMS/CAS), Nam Co Monitoring and Research Station for Multisphere Interactions (hereinafter Nam Co), Linzhi Station for Alpine Environment Observation and Research (hereinafter Linzhi station), and Maqu station. The locations of the four sites are shown in Fig. 1. The detailed coordinates and elevations of the sites are

TABLE 1. Eddy-covariance site information and parameters used in TK2.

	QOMS/CAS	Nam Co	Linzhi	Maqu
Lat	28°21.63′N	30°46.44′N	29°45.96′N	33°53.23′N
Lon	86°56.93′E	90°59.31′E	94°44.32′E	102°8.44′E
Elev (m)	4276	4730	3327	3439
Eddy-covariance measurement height (m)	3.1	3.3	3.1	3.5
Direction of LI-7500 (°)	135	194	105	—
Horizontal distance (CSAT3–LI-7500) (m)	0.23	0.29	0.18	0.15
Direction of CSAT3 (°)	180	150	285	—
Sample frequency (Hz)	10	10	10	10

listed in Table 1. The first three stations were established by the Institute of Tibetan Plateau Research of the Chinese Academy of Sciences (Ma et al. 2008a). Maqu station was built by the Cold and Arid Regions Environmental and Engineering Research Institute of the Chinese Academy of Sciences. These sites are essentially flat and are covered with very sparse and short grass in the monsoon season.

QOMS/CAS is located 30 km from Mount Everest. The dataset of the QOMS/CAS station consists of surface radiation components (Kipp and Zonen, Inc., model CNR-1); vertical profiles of air temperature, humidity, wind speed and direction (Vaisala, Inc., model MILOS520); and turbulent fluxes. Sensors for wind speed, wind direction, air temperature, and relative humidity are installed at five different levels (1.0, 2.0, 4.0, 10.0, and 20.0 m) on a 40-m PBL tower. An open-path eddy-covariance turbulent measurement system (Campbell Scientific, Inc., model CSAT3–Li-Cor, Inc., model LI-7500) is set up at 3.5-m height and runs continuously at a sampling frequency of 10 Hz. A dataset covering 1 April–31 December 2007 was used in this paper. The surface of the site is formed by sandy soil with small rocks. Sparse vegetation up to 0.2 m in height is found scattered around the station in summertime.

The surface at Nam Co is relatively smooth and is covered with very sparse and short grass in the monsoon season. The meteorological measurements (sensor height, depth, and types) taken at Nam Co and QOMS/CAS are the same (http://www.namco.itpcas.ac.cn/namcoenglish.html). During winter, the station surface is continuously covered by a homogeneous, flat, and open snow field. To test the applicability of the heat-parameterization method over snow, we ran SEBS with observation data from a snow-covered period at Nam Co station.

Linzhi station is located in the southeast of the Tibetan Plateau. The site's surface is mainly covered with a dense canopy, and the site is surrounded by forest. This canopy is the highest and densest of the four sites, as displayed by the high normalized difference vegetation index (NDVI) values in Fig. 2. The meteorological sensors are the same as those at QOMS/CAS and Nam Co. A dataset covering 25 February–30 October 2007 was used from this site for the study.

Maqu station is located on the northeast side of the Tibetan Plateau. The Maqu site has a relatively smooth surface and is covered with short grass in the monsoon season. Sensors of wind speed, wind direction, air temperature, and relative humidity are installed at five different levels (1.4, 3.2, 4.4, 8.4, and 18.4 m) on a PBL tower. Four components of radiation (CNR-1) are installed 1.5 m above ground. Meteorological measurements from each station used in this study have been listed in Table 2.

b. Data processing

Before using turbulent fluxes of the eddy-covariance system, a data-quality assessment and controlling process was applied to the turbulent data. From the high-quality dataset, we sought to find more suitable parameterization methods for the plateau land-cover types.

The high-frequency turbulence data were processed to produce half-hourly fluxes. Calibrations of the eddy-covariance signals were also executed. Meteorological and soil-observation data were sampled every 10 min.

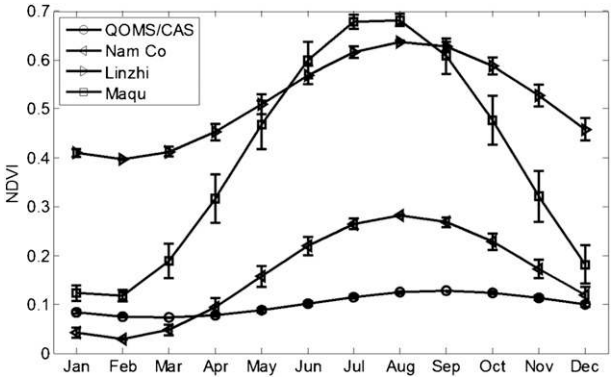

FIG. 2. Seasonal variation of NDVI at QOMS/CAS, Nam Co, Linzhi, and Maqu. Vertical lines represent the standard error bar.

TABLE 2. Meteorological measurements and parameters used to run SEBS. The WindSonic model is from Gill Instruments, Ltd. The models HMP45D and PTB220B are from Vaisala.

	QOMS/CAS	Nam Co	Linzhi	Maqu
Wind speed; wind direction	Height = 10.0 m; Vaisala	Height = 10.0 m; Vaisala	Height = 5.0 m; Vaisala	Height = 8.4 m; WindSonic
Air temperature and humidity	Height = 10.0 m; HMP45D	Height, 10.0 m; HMP45D	Height, 5.0 m; HMP45D	Height, 8.4 m; HMP45D
Surface radiation	CNR-1	CNR-1	CNR-1	CNR-1
Pressure	PTB220B	PTB220B	PTB220B	PTB220B
HC_{min} (m)	0.002	0.002	0.002	0.002
HC_{max} (m)	0.1	0.01	0.8	0.3
F	0.55	0.55	0.55	0.55
Time period	31 Mar–31 Dec 2007	5 Mar–15 Oct 2007	25 Feb–30 Oct 2007	10 May 2009–19 May 2010

All datasets were then resampled to 30-min intervals by nearest interpolation method. For all fluxes in this paper, the same sign convention is used: fluxes transporting energy toward the surface are negative, and fluxes transporting energy away from the surface are positive.

The application of the eddy-covariance technique is based on a few theoretical assumptions, such as horizontal homogeneity, steady-state conditions, and nonadvective conditions (Gockede et al. 2004). Therefore, to gain high-quality flux data, quality assessment and quality control have to be established in the processing of the eddy-covariance data. The TK2 software package (Mauder and Foken 2011) was used here to process the turbulent data of QOMS/CAS, Nam Co, and Linzhi. The spike-detection algorithm of Vickers and Mahrt (1997) was used to remove physically or electronically unfeasible values in the high-frequency turbulent data. The time delay between sonic-anemometer (CSAT3) and gas-analyzer (LI-7500) signals was eliminated by maximizing covariance. Tilt correction was done with the planar-fit method (Wilczak et al. 2001). Correction of spectral loss was done according to the Moore (1986) method. The sonic temperature was converted into actual temperature. The Webb–Pearman–Leuning (WPL) corrections (Webb et al. 1980) were also performed in the process. The TK2 input parameters of each eddy-covariance system are listed in Table 1.

The dataset for Maqu station has already been processed by Wang et al. (2012). Spike detection, the

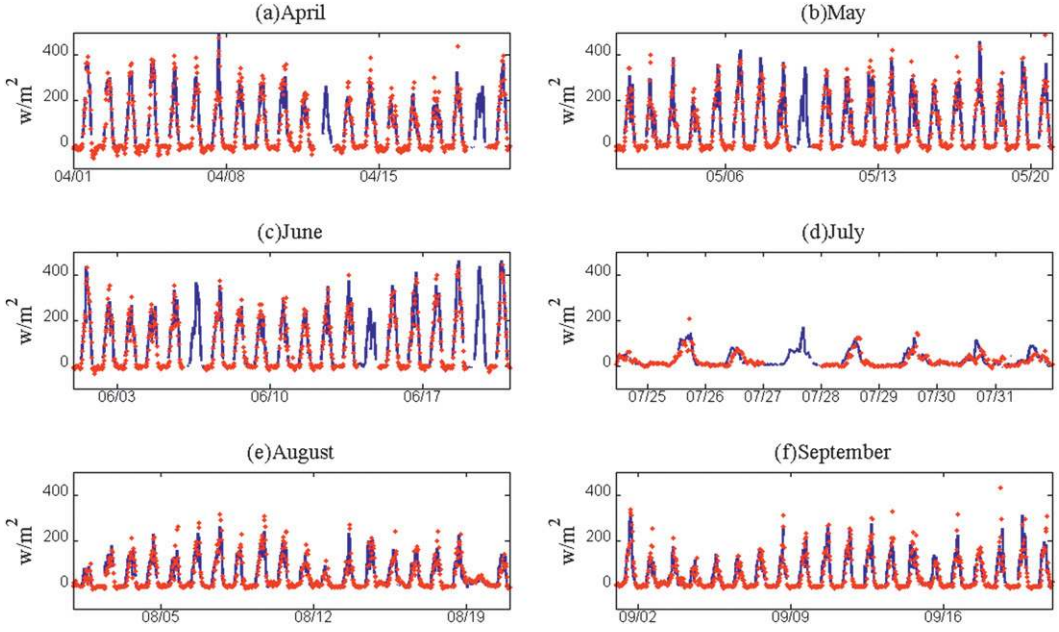

FIG. 3. Time series of observed sensible heat flux (blue line) and SEBS (Su02) output values (red points) at QOMS/CAS in 2007.

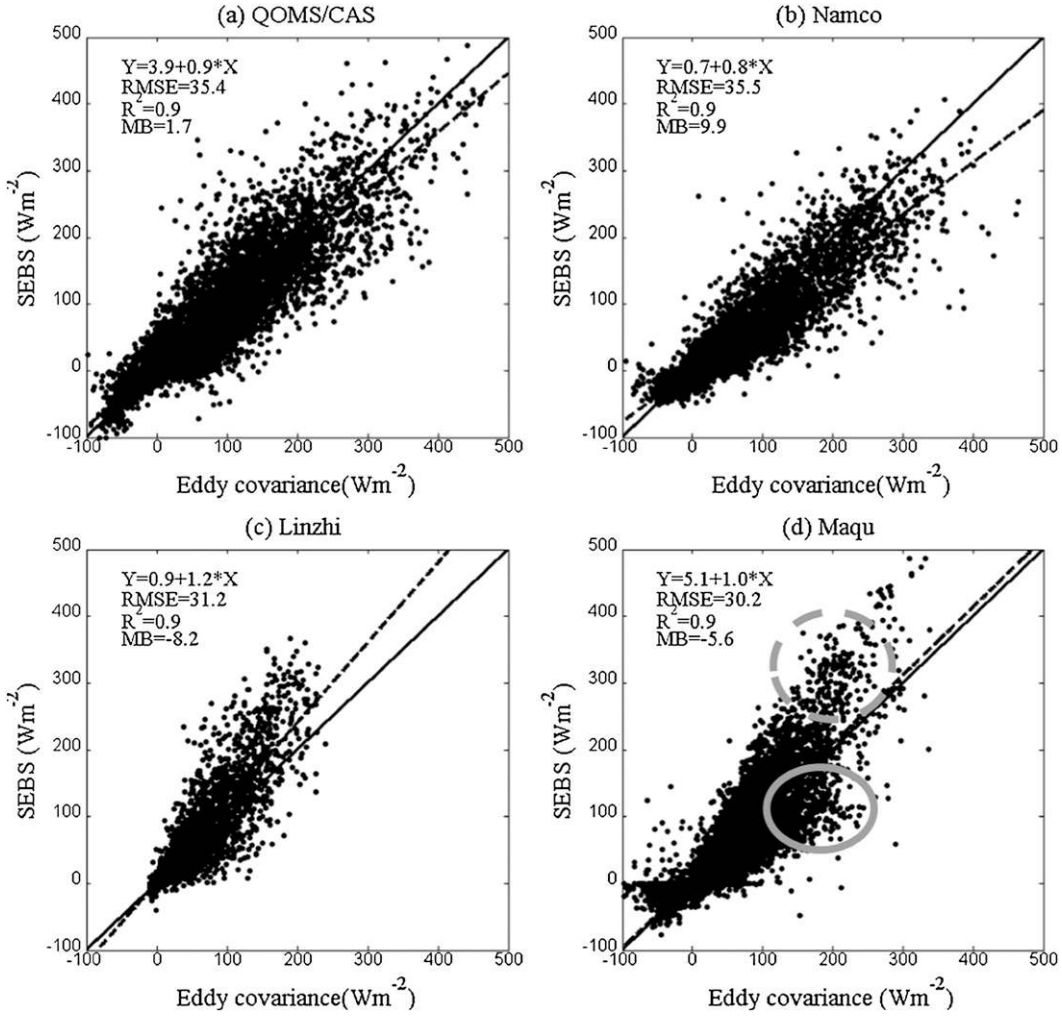

FIG. 4. Scatterplots of H (W m^{-2}) between the measurements of eddy covariance and outputs of SEBS (Su02) sensible heat flux data in 2007 at (a) QOMS/CAS, (b) Nam Co, (c) Linzhi, and (d) Maqu. The 1:1 and linear-fitting lines are shown by the solid and dashed lines, respectively.

two-rotation method (McMillen 1988), correction of spectral loss (Moore 1986), conversions of sonic temperature to actual temperature, and WPL corrections (Webb et al. 1980) were all performed. The quality of the sensible heat fluxes at the Maqu site is also controlled by manual inspection and consistency checks of overlapping or related measurements.

c. Local-scale evaluation and problem analysis

To run SEBS at a point scale, the air temperature, relative humidity, wind speed at 10-m height, land surface temperature (LST), pressure, and four-component radiation datasets from each station were used. The detailed information of the driven datasets is listed in Table 2. The LST was computed from measured upward longwave radiation (Rlwu) and downward longwave radiation (Rlwd) using the Stefan–Boltzmann equation:

$$\mathrm{Rlwu} = (1 - \varepsilon)\mathrm{Rlwd} + \varepsilon\sigma\mathrm{LST}^4, \tag{3}$$

where σ is the Stefan–Boltzmann constant (5.67×10^{-8} W m^{-2} K^{-4}). The emissivity ε was calculated from the NDVI, according to the method of Sobrino et al. (2004). The emissivity of a snow surface was set to 0.99. For an NDVI < 0.2, the land surface was considered to be bare soil, with $\varepsilon = 0.97$. For an NDVI > 0.5, the land surface was considered to be fully vegetated, with $\varepsilon = 0.99$. For $0.2 \leq \mathrm{NDVI} \leq 0.5$, ε was calculated according to

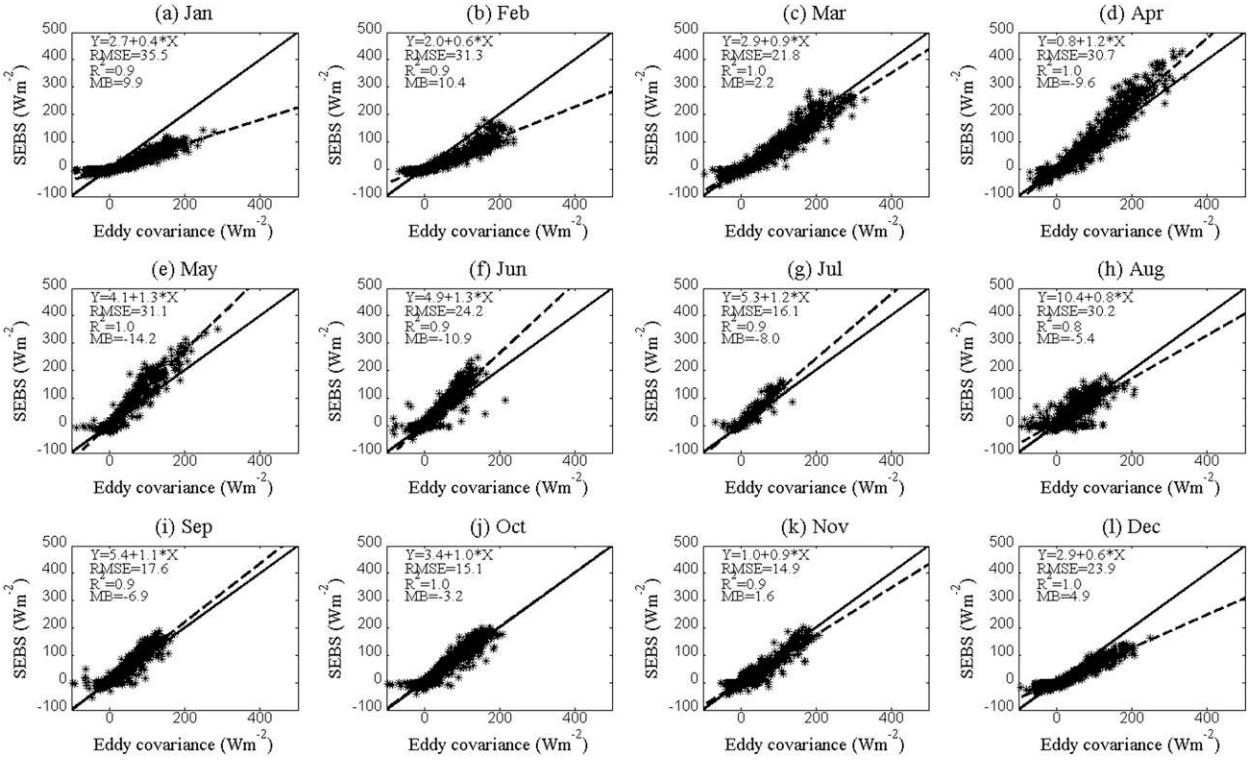

FIG. 5. As in Fig. 4, but for the individual months at Maqu.

$$\varepsilon = \varepsilon_v f_c + \varepsilon_s(1 - f_c) + (1 - \varepsilon_s)(1 - f_c)F\varepsilon_v, \qquad (4)$$

where ε_v is the emissivity of vegetation, ε_s is the bare-soil emissivity, the shape factor F is given a value of 0.55 (Sobrino et al. 2004), and canopy fraction

$$f_c = \frac{\text{NDVI} - \text{NDVImin}}{\text{NDVImax} - \text{NDVImin}}. \qquad (5)$$

The values of NDVImin and NDVImax are approximately 0.2 and 0.5, respectively (Sobrino et al. 2004). For an NDVI < 0.2, $f_c = 10^{-5}$, and for an NDVI > 0.5, $f_c = 1$. The time series of NDVI was collected from the Système Pour l'Observation de la Terre (SPOT) "VEGETATION ten daily synthesis archive" NDVI products (http://free.vgt.vito.be/) and was processed by the Harmonic Analysis of Time Series (HANTS) model (Verhoef et al. 1996) to eliminate cloud noise. The monthly average of the NDVI at the four stations is depicted in Fig. 2.

The SEBS model was run to produce accurate sensible heat flux results, which was achieved by using available observational variables. All of the observed variables used to run SEBS are listed in Table 2. The time period of each station is also shown in Table 2. Both simulated and observed values of sensible heat flux at QOMS/CAS are shown in Fig. 3. The observations from April to September of 2007 were used to evaluate the performance of SEBS at the site. This extensive dataset provides a good sample of the local climatological conditions and different atmospheric stability conditions. Measurements are considered to be "true" values after careful calibration and quality control by TK2. The results in Fig. 3 demonstrate that SEBS can capture the diurnal and seasonal variations of sensible heat flux very well when driven by a sound dataset. The results of the other three stations are similar to those of the first and are not depicted here.

The scatterplots in Fig. 4 show that most of the points are located around the 1:1 line. The results of the statistical analysis are also listed in each panel. The root-mean-square error (RMSE) and the mean bias (MB) were respectively calculated as

$$\text{RMSE} = \left[\sum_{i=1}^{N} (\text{obs}_i - x_i)^2/N\right]^{1/2} \quad \text{and} \qquad (6a)$$

$$\text{MB} = \frac{1}{N}\sum_{i=1}^{N} (\text{obs}_i - x_i), \qquad (6b)$$

where x_i is a simulation of SEBS, obs_i is an observation, and N is the sample number.

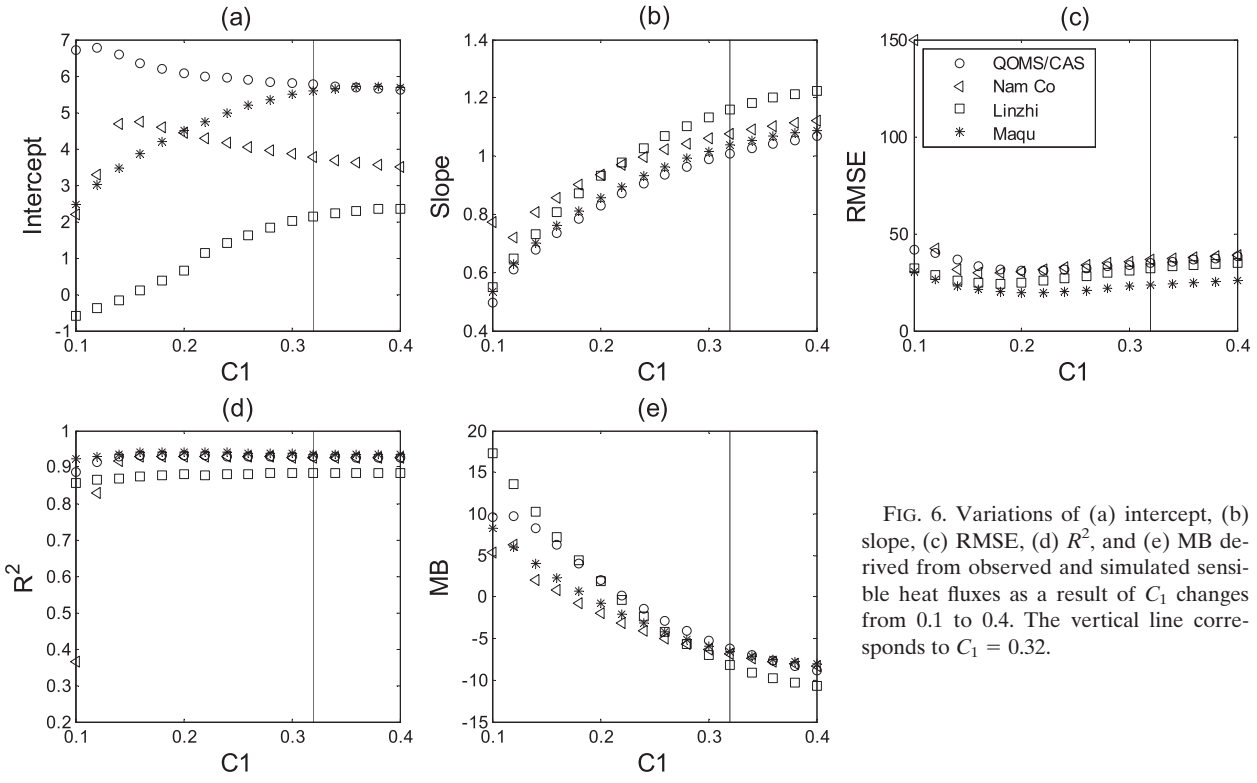

FIG. 6. Variations of (a) intercept, (b) slope, (c) RMSE, (d) R^2, and (e) MB derived from observed and simulated sensible heat fluxes as a result of C_1 changes from 0.1 to 0.4. The vertical line corresponds to $C_1 = 0.32$.

The result shows that RMSE changes from 30 to 35 W m^{-2}, all of the correlation coefficients squared R^2 are higher than 0.9, and MB is below 9.2 W m^{-2}. The linear-fitting line is depicted by a dashed line in Fig. 4. The slopes in Fig. 4 demonstrate that SEBS produces a slightly lower estimation of sensible heat flux at QOMS/CAS and Nam Co. Figures 4c and 4d show some sensible heat fluxes simulated by SEBS to be systematically higher than the observations (see the dashed circle) while others are systematically lower (see the solid circle). Even with these systematic deviations in Figs. 4c and 4d, the fitting line and statistical results are still comparable with Figs. 4a and 4b. To find during which period the estimations are lower or higher, the scatter-point distribution of each month for Maqu is redrawn in Fig. 5, demonstrating that the simulation values for January, February, and December are lower than the observations whereas the values for April, May, June, and July are a bit higher. Underestimation of sensible heat flux has been reported in results by Van der Kwast et al. (2009) and Yang et al. (2010). Overestimation of sensible heat flux has not been reported to date. Next, we try to identify the most critical factor in the determination of sensible heat flux and propose a practical solution.

3. Method and results

a. Sensitivity analysis

To calculate the sensible heat flux by means of a similarity theory, the roughness height for heat transfer must be accurately determined. The primary objective of this study is to evaluate the roughness-height-parameterization method for heat transfer in SEBS over the Tibetan Plateau. The scalar roughness height for heat transfer z_{0h} can be derived from the following equations:

$$\beta = C_1 - C_2 \exp(-C_3 C_d \times \mathrm{LAI}), \tag{7a}$$

$$n_{\mathrm{ec}} = (C_d \times \mathrm{LAI})/(2\beta), \tag{7b}$$

$$d_0/\mathrm{HC} = 1 - \frac{1}{2n_{ec}}[1 - \exp(-2n_{\mathrm{ec}})], \tag{7c}$$

$$z_{0m} = \mathrm{HC}[1 - (d_0/\mathrm{HC})]\exp(-k/\beta), \quad \text{and} \tag{7d}$$

$$z_{0h} = z_{0m}/\exp(kB^{-1}), \tag{7e}$$

where C_1, C_2, and C_3 are model constants related to the bulk surface drag coefficient (Massman 1997); LAI is leaf area index, derived from NDVI; C_d is the foliage drag

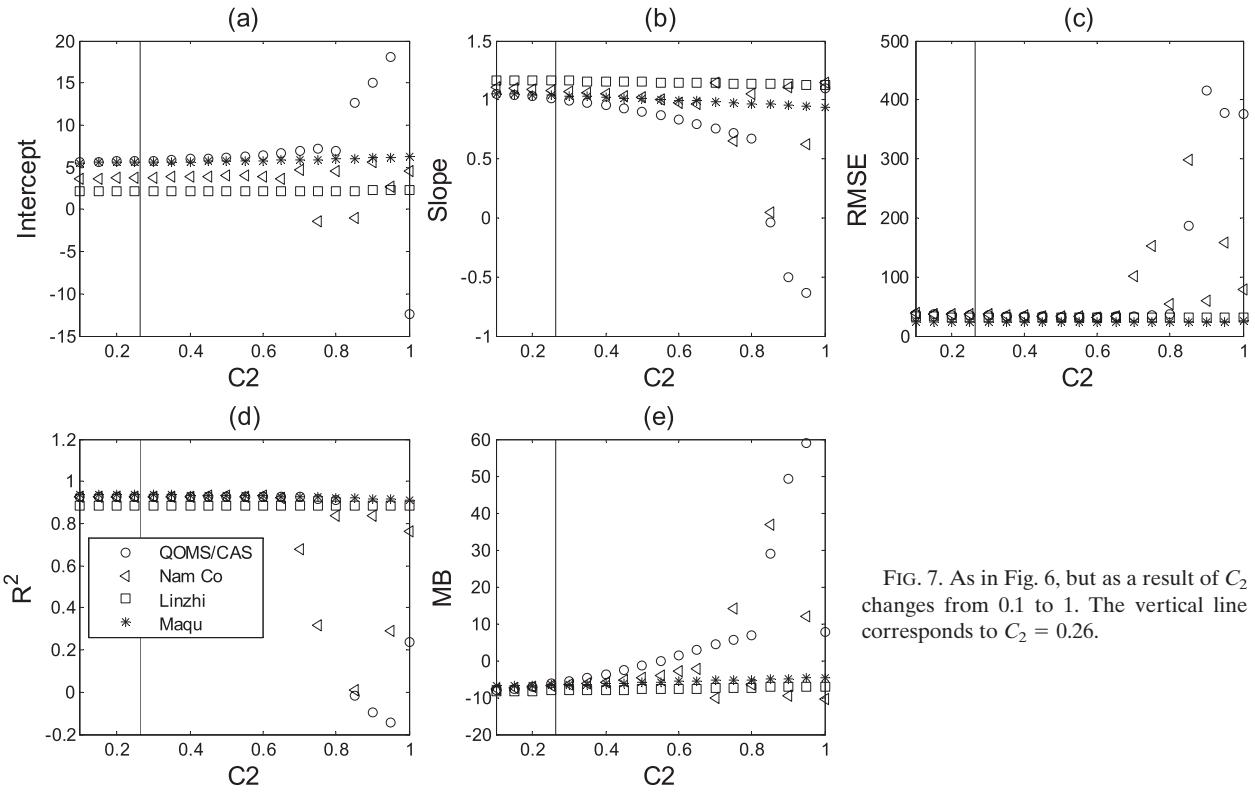

FIG. 7. As in Fig. 6, but as a result of C_2 changes from 0.1 to 1. The vertical line corresponds to $C_2 = 0.26$.

coefficient; n_{ec} is the wind speed profile extinction coefficient in the canopy; d_0 is the displacement height; z_{0m} is the roughness height for momentum transfer; k (=0.4) is the von Kármán constant; and HC is the height of the canopy (m), which is computed from NDVI by using

$$\mathrm{HC} = \mathrm{HC}_{\min} + \frac{\mathrm{HC}_{\max} - \mathrm{HC}_{\min}}{(\mathrm{NDVI}_{\max} - \mathrm{NDVI}_{\min})}(\mathrm{NDVI} - \mathrm{NDVI}_{\min}), \tag{8}$$

where $\mathrm{HC}_{\max}$ and $\mathrm{HC}_{\min}$ are the measured maximum and minimum canopy height, respectively; $\mathrm{HC}_{\min}$ is set to 0.0012, and $\mathrm{HC}_{\max}$ is the highest measured value for canopy height in 1 yr.

On the basis of fractional canopy coverage, Su (2002) presented kB^{-1} as follows (this method will be abbreviated as Su02 hereinafter):

$$kB^{-1} = f_c^2 kB_c^{-1} + f_s^2 kB_s^{-1} + 2f_c f_s kB_m^{-1}, \tag{9}$$

where f_c is the fractional canopy coverage and f_s is that of soil, kB_c^{-1} is the kB^{-1} of the canopy and kB_s^{-1} is that of bare soil, and kB_m^{-1} represents kB^{-1} for mixed bare soil and canopy.

From Eqs. (7a)–(7e), we can see that the uncertainties in C_1, C_2, C_3, C_d, HC, and NDVI directly influence d_0, z_{0m}, and z_{0h}, which will ultimately determine the accuracy of canopy turbulent flux simulations. The values of C_1, C_2, C_3, and C_d have been given by Massman (1997) to parameterize the surface drag coefficient. To date, nobody has tested the applicability of these values over the Tibetan Plateau canopy. Variations in the fitting line's slope and intercept, RMSE, R^2, and MB in predicted heat fluxes with C_1, C_2, C_3, and C_d are given in Figs. 6–9, respectively. Here, we use the eddy-covariance observed turbulent fluxes as reference. The slope and intercept, RMSE, R^2, and MB for all four sites are plotted to analyze their influence on sensible heat flux for different environments and land surfaces. Figure 6 shows that the slope can increase from 0.5 to 1.2 while RMSE and R^2 vary little when C_1 increases from 0.15 to 0.4. The intercept becomes stable when C_1 is above 0.32. Most of the MB values are negative, which means increasing or decreasing C_1 will not solve the problem in Fig. 4. Bache (1986) suggests that C_1 varies between 0.15 and 0.4 for different canopy types. From the sensitivity evaluations, we suggest that the value of C_1 not be adjusted. The results in Fig. 7 demonstrate that all five variables vary little regardless of changes in C_2. This outcome shows that C_2 is not a principal parameter, and

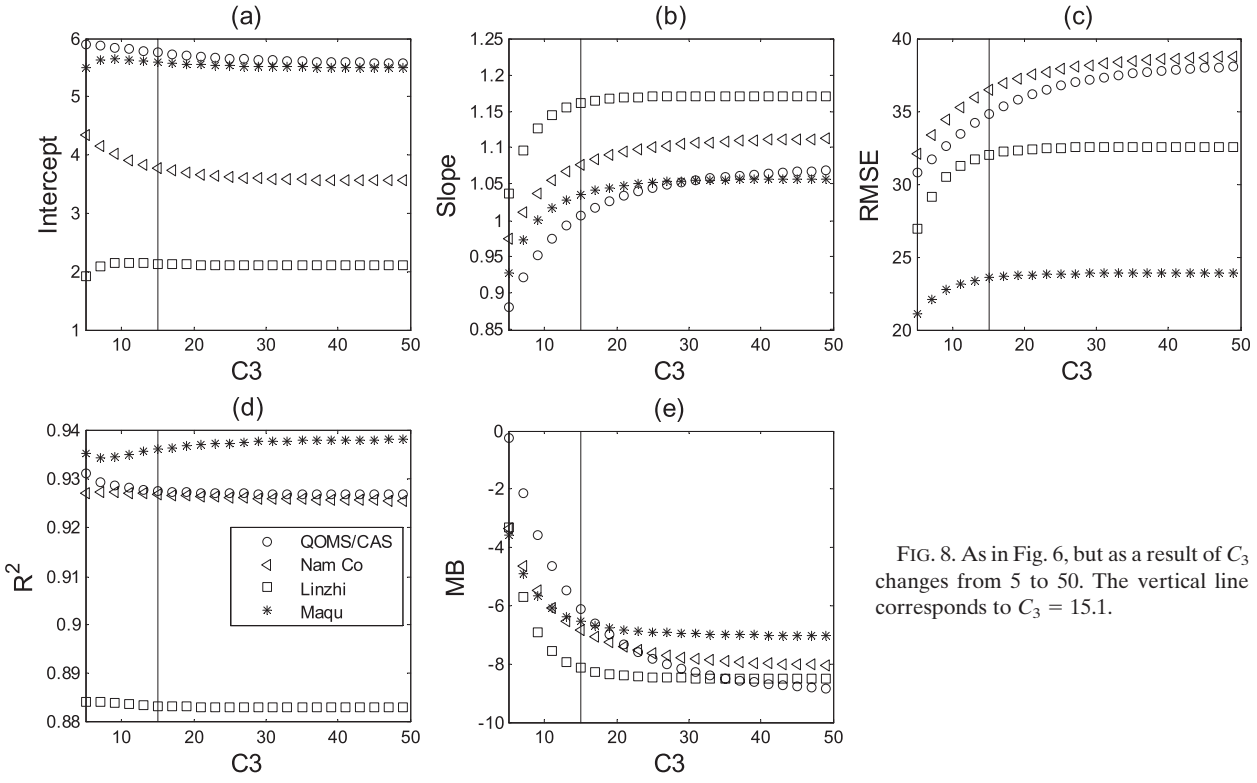

FIG. 8. As in Fig. 6, but as a result of C_3 changes from 5 to 50. The vertical line corresponds to $C_3 = 15.1$.

therefore its original value has not been altered. For C_3, the intercept and R^2 change little with changes in C_3 whereas slope, RMSE, and MB are sensitive to C_3 changes when C_3 falls below 15. On the other hand, when C_3 is above 15, the statistical variables become stable. The values of slope may change with C_3 while the MB remains negative. This relationship means that there are more points distributed below the 1:1 line. This result also displays the inability to solve problems related to the SEBS sensible heat flux by adjusting C_3. From the above sensitivity analysis of the five statistical variables, the original values of $C_1 = 0.32$, $C_2 = 0.26$, and $C_3 = 15.1$ have been used here. We believe they are suitable for the canopy of the Tibetan Plateau.

The foliage drag coefficient C_d as a function of height within the canopy is assumed to be uniform throughout the low canopy. The influence of C_d on the five statistical variables was estimated, as shown in Fig. 9. At Nam Co all five variables changed little with C_d. The slopes were around 0.75, and the average MB was 10 W m^{-2}. Therefore, changing C_d will not resolve the lower H estimation problem in SEBS at Nam Co. When C_d increased from 0.1 to 0.5, the slope of QOMS/CAS was enhanced from 0.75 to 0.92 and the MB was reduced to zero. Thus, C_d changes can solve the problem of SEBS at QOMS/CAS. The MB values at Linzhi and Maqu were still negative when C_d was increased. The slopes at Linzhi and Maqu decreased persistently from 1.2 and 1, respectively, with increasing C_d. From these results, we can see that increasing C_d has a different impact on the four stations' slope and MB results. This study disclosed that the lower estimation of sensible heat flux at Nam Co (discussed in section 2c) is not caused by the C_d value whereas for the dense canopies at Linzhi and Maqu the influence of C_d becomes important. From these sensitivity analyses, we can conclude that the systematic errors in the SEBS sensible heat flux at the four stations cannot be solved by adjusting the values of C_1, C_2, C_3, and C_d.

Van der Kwast et al. (2009) have pointed out that the canopy height HC can cause large deviations in the modeling of sensible heat flux. As shown in Eq. (8), the magnitude of HC is determined by HC_{max} and NDVI. The constant HC_{max} was also included in the sensitivity analysis, and the results are presented in Fig. 10. All of the slope values at the four stations increased from below 1 to above 1, and the MB values decreased from positive to negative with increasing canopy height. Figure 10 reveals that the accuracy of the estimated canopy height is important for the final fluxes. This can be settled by measuring the height of the canopy. The measured HC_{max} values that have been used in SEBS are listed in Table 2. The sensitivity test of HC_{max} can also be used to appraise the measured canopy height. The practical

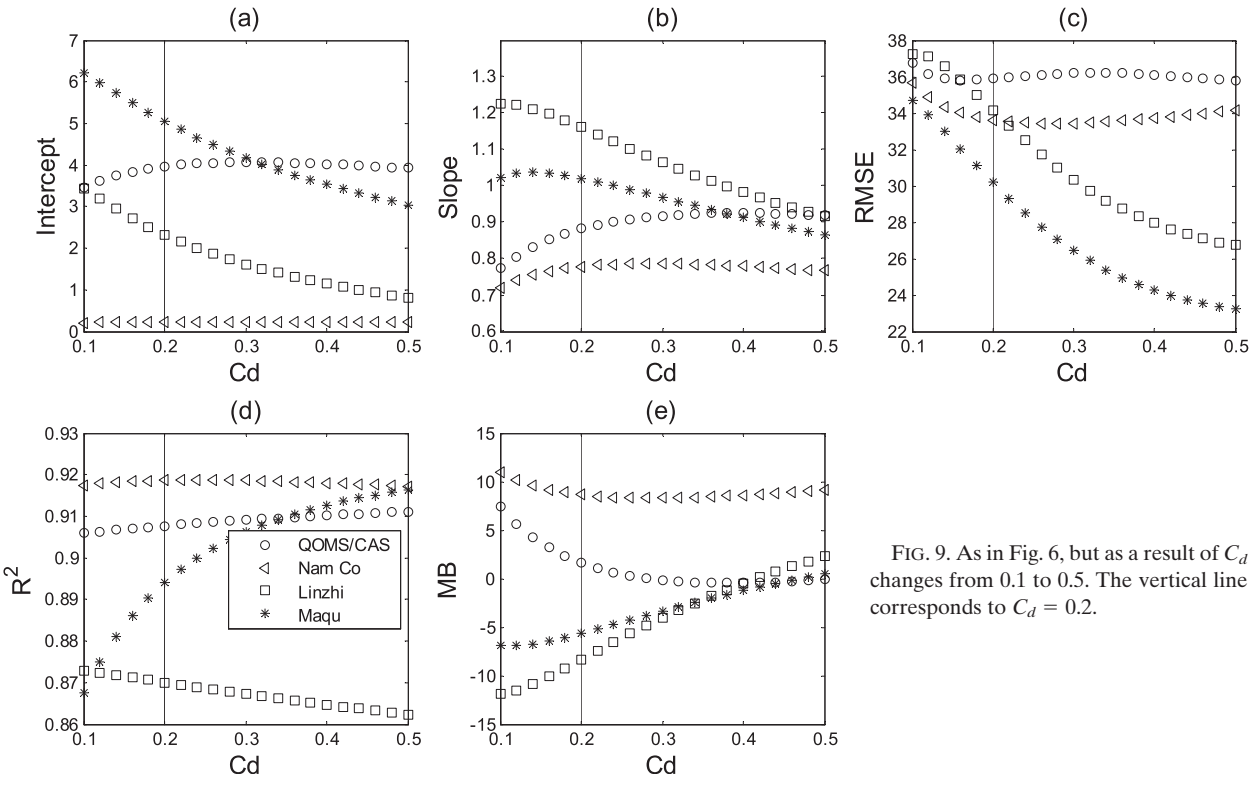

FIG. 9. As in Fig. 6, but as a result of C_d changes from 0.1 to 0.5. The vertical line corresponds to $C_d = 0.2$.

canopy height has been estimated by in situ site inspection and was used in this study. Thus, HC_{max} cannot trigger SEBS to produce sensible heat flux bias. Because other variables, such as NDVI, LAI, wind speed, and air temperature, are also taken from measurements, we assume their accuracy is influenced by the equipment. Their sensitivity will not be discussed further. A final option rests with the parameterization of kB^{-1}.

b. Improvement of roughness height for heat transfer

From Fig. 5, we can see that lower estimation of sensible heat fluxes occurred during winter. From the time series comparison analysis, the significant lower estimations were during the daytime. A diurnal pattern exists in the difference between observed and simulated sensible heat fluxes. In Eq. (9), kB^{-1} was divided into three parts: bare soil, canopy, and mixed canopy and soil. In winter, coverage of the land surface was dominated by bare soil. The role of bare soil, kB_s^{-1}, should be the most important part. As a test over the bare soil of the Tibetan Plateau (Chen et al. 2010; Zhang 2010), the heat roughness height parameterization method of Yang et al. (2002) was introduced into the kB^{-1} of SEBS (this method will be abbreviated as SY02 hereinafter). The kB_s^{-1} of bare soil in Eq. (9) was revised according to

$$z_{0h} = (70\vartheta/u_*)\exp(-7.2u_*^{0.5}\theta_*^{0.25}) \quad \text{and} \quad (10a)$$

$$kB_s^{-1} = \log(z_{0m}/z_{0h}), \quad (10b)$$

where ϑ is the kinematic viscosity of air (1.5×10^{-5} m^2 s^{-1}), u_* is the surface friction velocity (m s^{-1}), and θ_* is the surface friction temperature (K).

Several studies have discussed the diurnal change in kB^{-1} over the Tibetan Plateau (Ma et al. 2009; Wang and Ma 2011). Because z_{0h} is computed with u_* and θ_*, in Eq. (10a), and u_* and θ_* have diurnal change information, this will first be transported to z_{0h}, and then to kB^{-1}. The diurnal change information of z_{0h} and kB^{-1} is important in the calculation of surface flux through z_{0h} or kB^{-1} in MOST. This makes the kB_s^{-1} value in Eq. (10b) better than the fixed kB_s^{-1} value of Eq. (9). After upgrading kB_s^{-1} in SEBS [kB_c^{-1} and kB_m^{-1} are the same as in Su et al. (2001)], the results are depicted in Figs. 11 and 12. The statistical variables before and after the improvement are all listed in Table 3 for comparison. The scatter distributions in Fig. 11 are closer to the 1:1 line than in Fig. 4. The monthly scatterplots for Maqu station also demonstrate an enhancement in SEBS performance during wintertime.

After introduction of the equation of z_{0h} by Yang et al. (2002), the linear fitting lines are situated closer to

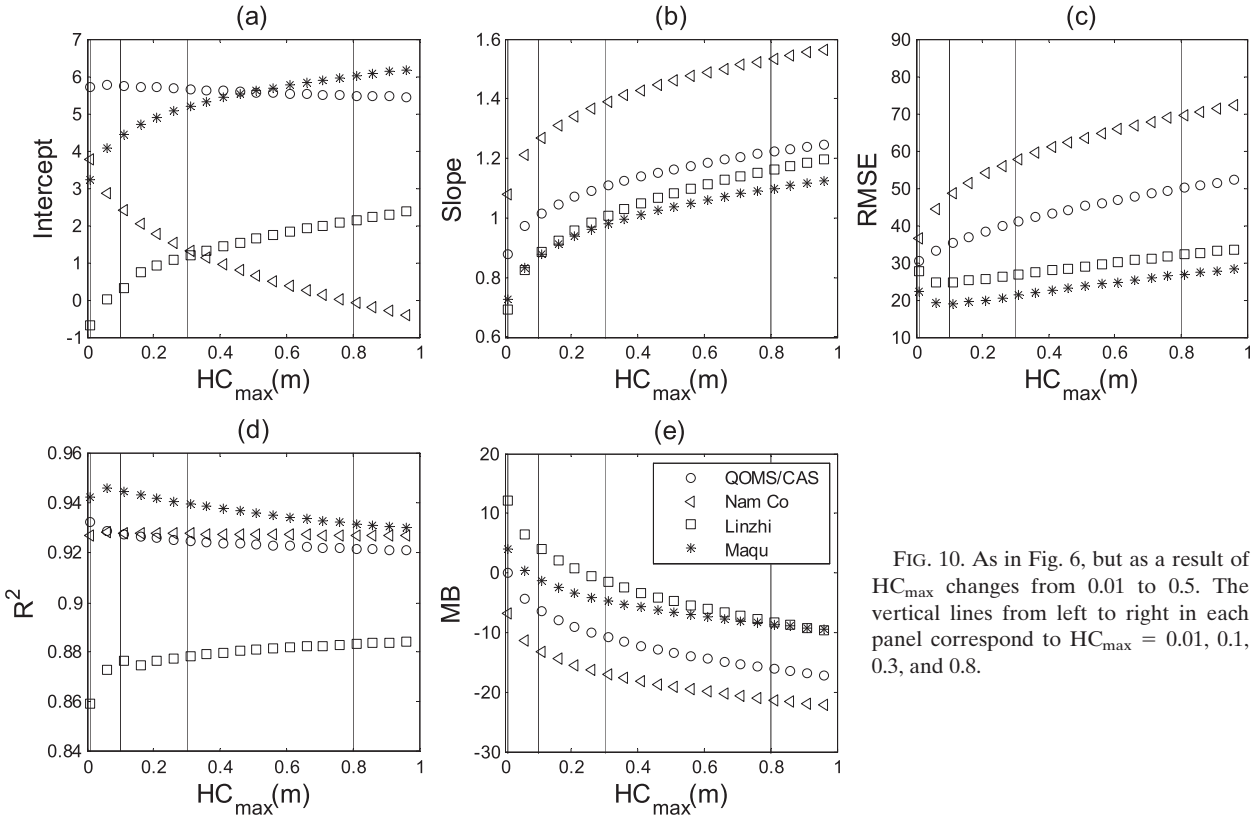

FIG. 10. As in Fig. 6, but as a result of HC_{max} changes from 0.01 to 0.5. The vertical lines from left to right in each panel correspond to HC_{max} = 0.01, 0.1, 0.3, and 0.8.

the 1:1 line. Other statistical values show little change. The results show better performance of the new kB^{-1}. We conclude that the method is preferable for the Tibetan Plateau.

c. *Further test of the kB^{-1} scheme for the Tibetan Plateau snow surface*

For the snow surface, where f_c is equal to 0, Eqs. (10a) and (10b) will be used to compute sensible heat flux according to Eq. (8) after revision. The z_{0m} for a snow surface is given a value of 0.0001 (Arck and Scherer 2002). A snow depth of 0.4 m was manually measured between 25 November and 31 December 2006, at Nam Co station. The measurements during this period were used to evaluate the performance of SY02 for the snow surface (Figs. 13 and 14). The atmospheric surface layer over snow-covered land is often dominated by a very stable stratified layer. Under stable atmospheric stratification, turbulent events are intermittent. The intermittence of the turbulence causes violations of the eddy-covariance assumptions (steady-state conditions and flux-variance similarity) and yields a significant misestimation of the sensible heat flux (Lüers and Bareiss 2010). It is well documented that stable atmospheric stratification presents numerous challenges to the interpretation of surface fluxes that were measured using the eddy-covariance technique (e.g., Aubinet 2008; Helgason and Pomeroy 2011). In our study, we also found abnormal turbulent fluxes measured by the eddy covariance over the snow surface. Especially in cases of calm wind, most of the measured fluxes were abnormal. Measuring eddy covariance is more difficult during very stable air temperature stratification, low heat fluxes, and low wind velocities (Foken and Wichura 1996; Marks et al. 2008). When a gust of wind occurs, indicated by periods of yellow background in Fig. 13, the mechanical turbulence caused by the wind shear assists the heat exchange from the air to the snow. It may also increase the depth of the surface layer, which rises to above the sensors of the eddy covariance. During such disturbance periods, sensible heat fluxes measured by eddy covariance become reasonable. To obtain good-quality data, we set a standard of friction velocity > 0.2 m s^{-1} to determine time periods of strong wind shear. Selected data of eddy covariance were used to make a comparison with the values simulated by SEBS. The scatter points and fitting line are shown in Fig. 14. This result testifies to the validity of the roughness height presented here for heat transfer over a snow surface. Guo et al. (2011) also supported the reliable sensible heat flux

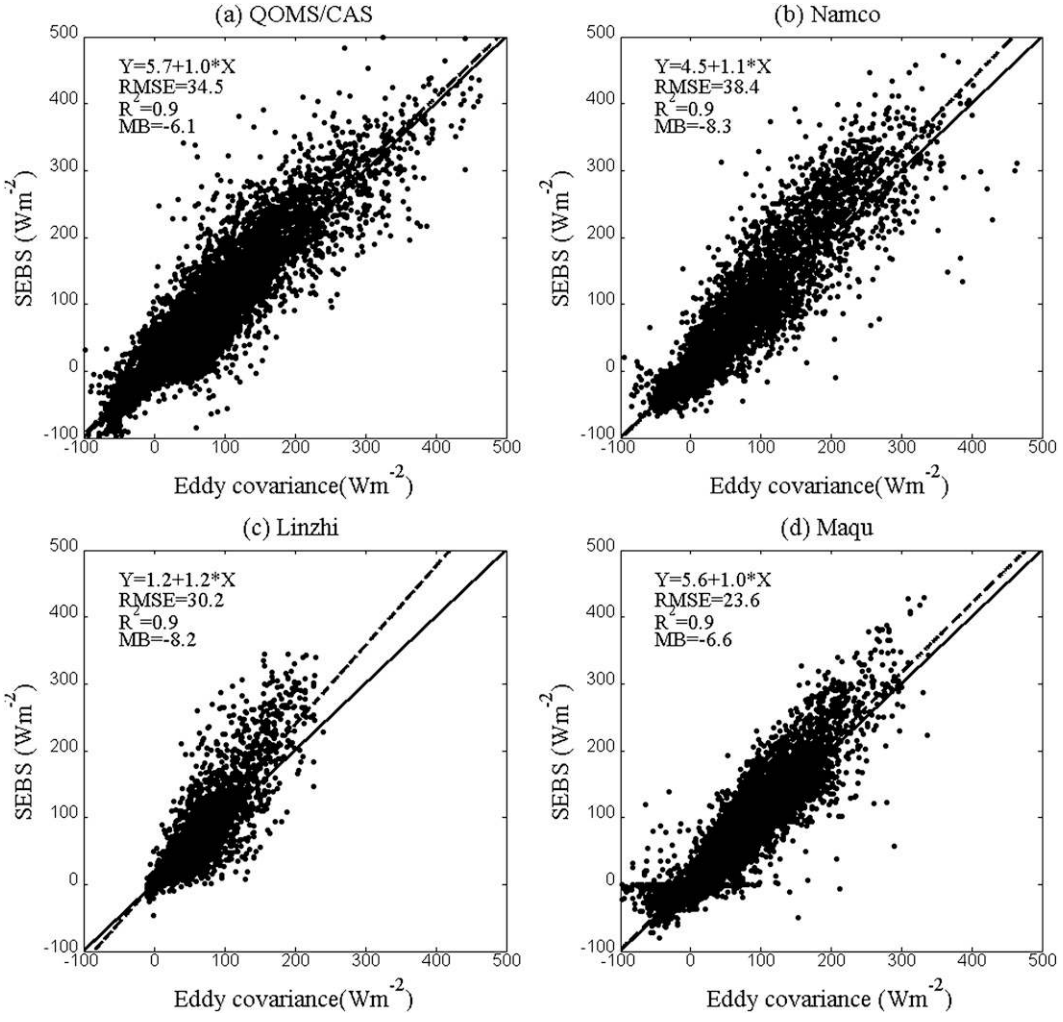

FIG. 11. Scatterplot of H (W m^{-2}) between the measurements of eddy covariance and outputs of SEBS (SY02) sensible heat flux data in 2007 at (a) QOMS/CAS, (b) Nam Co, (c) Linzhi, and (d) Maqu. The other items are similar to those in Fig. 4.

estimated with Yang et al.'s (2002) method over the snow surface of a Tibetan glacier snow surface. All these results indicate that our new revised heat parameterization is superior when applied to the Tibetan Plateau's bare soil or canopy, or even its snow surface.

4. Discussion and conclusions

In this study, SEBS was driven by a time series of meteorological observation data at point scales. The performance of SEBS has been evaluated by comparisons between its simulated sensible heat fluxes and a high-quality dataset of observed turbulent fluxes. The measurements were performed over typical Tibetan land-cover units. The results show that SEBS captured the diurnal and seasonal variations of sensible heat flux well, but they also show that the Su02 formulation of kB^{-1} tends to produce lower estimates for sensible heat flux over bare soil. Using sensitivity analyses, we have identified the most critical factor in the determination of effective roughness height. The wind speed profile extinction coefficient within the canopy proposed by Massman (1997) is applicable over the Tibetan Plateau canopy structure. The practical solution to replace the soil part of the kB^{-1} parameterization with the one by Yang et al. (2002) was proposed. The new parameterization equation of kB^{-1} in SEBS has been tested and was found to be an improvement over the original for bare soil and low canopies. Observations also evaluated the validity of the new heat roughness height parameterization of kB^{-1}over snow surfaces. The revised heat roughness length parameterization provides SEBS with

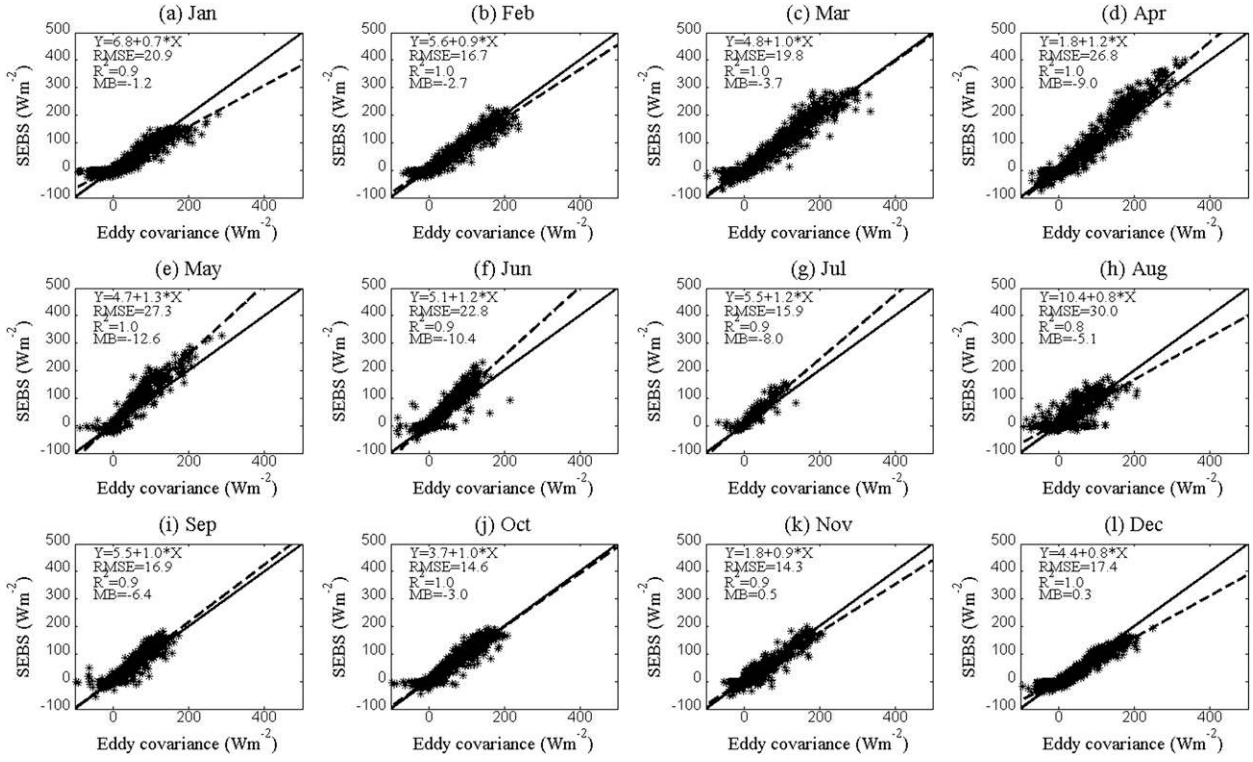

FIG. 12. As in Fig. 11, but for the individual months at Maqu.

improved accuracy and applicability over complex surfaces. The new scheme of turbulent heat flux parameterization method will be useful for land-surface interactions in the Tibetan Plateau climate models. This work helps to improve applicability of the model over typical land covers of the Tibetan Plateau and helps us to analyze the possibility and suitability of SEBS for generating surface turbulent heat flux maps over the whole plateau area by remote sensing techniques. Evaluated here over different land surface types, the sensible heat parameterization method can also be used in other regions of the Tibetan Plateau. It is also worth assessing the generality of the approach presented here for other regions. Whether the new kB^{-1} will benefit estimation of latent heat flux, which is derived as the residual of the surface energy balance in SEBS, needs further evaluation.

In practice, kB^{-1} was derived from the bulk transfer formulation using measurements of other quantities. Any uncertainties associated with these measurements will cause uncertainties in the evaluation of kB^{-1} and the final estimated sensible heat flux. The flux and meteorological variables may have different upwind source areas as a result of different measurement heights. This also explains the scatter points in Figs. 4 and 11. The surface temperature was determined using radiometers with a limited field of view. An assumption was made to regard this temperature as representative of the eddy-covariance system's fetch area. The discrepancy shown by the scatter points is believed to be related to

TABLE 3. Statistics results for simulated and observed sensible heat flux.

	QOMS/CAS		Nam Co		Linzhi		Maqu	
	Su02	SY02	Su02	SY02	Su02	SY02	Su02	SY02
Slope	0.9	1.0	0.8	1.1	1.2	1.2	1.0	1.0
Intercept (W m^{-2})	3.9	5.7	0.7	4.5	0.9	1.2	5.1	5.6
RMSE (W m^{-2})	35.4	34.5	35.5	38.4	31.2	30.2	30.2	23.6
R^2	0.9	0.9	0.9	0.9	0.9	0.9	0.9	0.9
MB (W m^{-2})	1.7	−6.1	9.9	−8.3	−8.2	−8.2	−5.6	−6.6

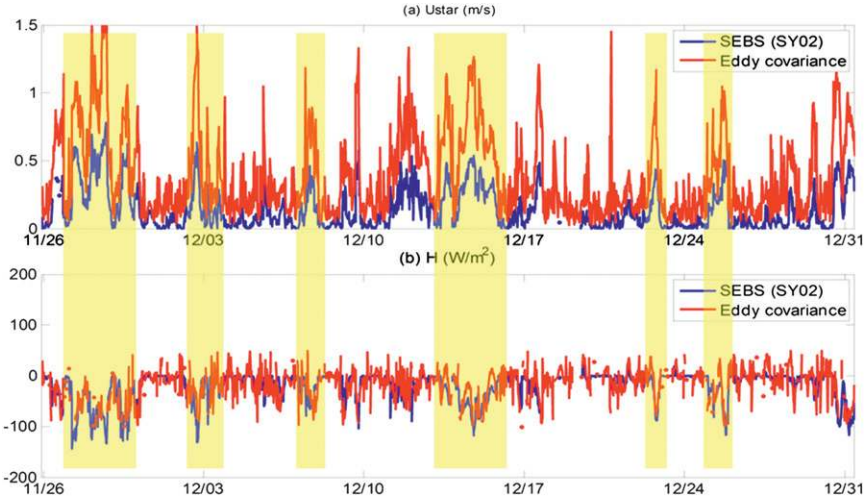

FIG. 13. Comparison of (a) friction velocity (m s^{-1}) and (b) sensible heat flux (W m^{-2}) between eddy covariance and SEBS (SY02) from 26 Nov to 31 Dec 2006, at the Nam Co site when the land surface is covered by snow. The periods with a yellow background provide a good comparison between SEBS (SY02) and eddy-covariance measurements.

differences in the footprints of the sensors and to effects of the inhomogeneous terrain.

The new kB^{-1} can only use diurnal information from meteorological measurements, because most satellites with high resolution provide us with one observation per day or per several days. This fact limits its usage in satellite applications.

SEBS has lower estimated momentum flux over the snow cover. This can be explained from the fact that it was given an ideal roughness length value of flat snow cover. In actual fact, the constructions around the measurement can also influence its representative value.

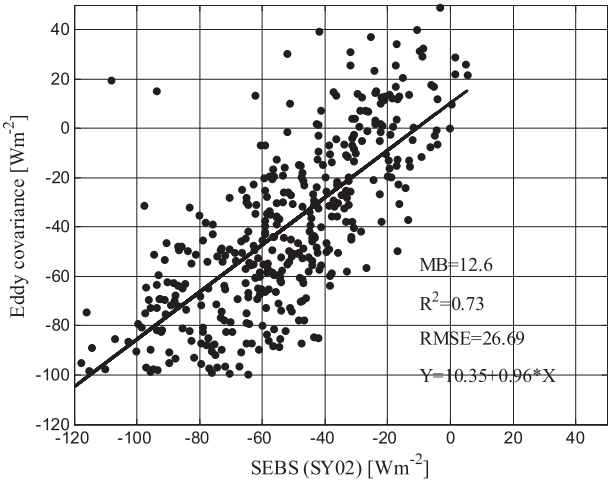

FIG. 14. Scatterplot and linear fitting of sensible heat flux (W m^{-2}) at the Nam Co site between eddy covariance and SEBS (SY02). The other items are similar to those in Fig. 4.

The roughness length in the direction of a building on site is bigger than the preestablished value in the model (Fig. 5 in Zhou et al. 2010). The heterogeneity of the land surface around the eddy-covariance device makes the actual roughness bigger than the ideal snow roughness length. Second, MOST uses an iterative scheme to calculate sensible heat flux. The initial value of u_* is that of neutral conditions, without stability correction. The initial value is already lower than the true value. All these factors explain why the simulated momentum flux is lower than the observations. Here, we revised the method for heat roughness length, which also is dependent on stability. Improvement of the stability-dependent profile functions in MOST may also help us to get more accurate surface fluxes.

This contribution also points out that canopy height is vital for turbulent heat simulations. The maximum and minimum canopy heights should be adjusted according to local observations. The results also demonstrate the inability of eddy covariance to obtain a useful flux observation in cases of calm winds over a snow surface.

Acknowledgments. This research was funded in part by the Chinese National Key Programme for Developing Basic Sciences (2010CB951701), the National Natural Science Foundation of China (40825015), the ESA-MOST Dragon I/II programme (Drought Monitoring, Prediction and Adaptation under Climatic Changes Project and Young Scientists Support), the European Commission CEOP–AEGIS project (Call FP7-ENV-2007-1 Grant 212921; information online at http://www.ceop-aegis.org/), and the ESA STSE WACMOS project

(www.wacmos.org). Xuelong Chen is supported by the CAS-KNAW Joint PhD Training Programme. The authors thank all members of QOMS/CAS for their extensive assistance with the field observations for this research. We thank Prof. Thomas Foken for discussions. The authors thank all of their colleagues for their very hard work in the construction and field work at the Tibetan Observation and Research Platform (TORP). The dataset for the Maqu station was provided and processed by the Zoige Plateau Wetlands Ecosystem Research Station.

REFERENCES

Arck, M., and D. Scherer, 2002: Problems in the determination of sensible heat flux over snow. *Geogr. Ann.,* **84A,** 157–169.

Aubinet, M., 2008: Eddy covariance CO_2 flux measurements in nocturnal conditions: An analysis of the problem. *Ecol. Appl.,* **18,** 1368–1378, doi:10.1890/06-1336.1.

Bache, D. H., 1986: Momentum transfer to plant canopies: Influence of structure and variable drag. *Atmos. Environ.,* **20,** 1369–1378.

Beljaars, A. C. M., and A. A. M. Holtslag, 1991: Flux parameterization over land surfaces for atmospheric models. *J. Appl. Meteor.,* **30,** 327–341.

Brutsaert, W., Ed., 1982: *Evaporation into the Atmosphere: Theory, History, and Application.* D. Reidel, 299 pp.

Chen, Y., K. Yang, D. Zhou, J. Qin, and X. Guo, 2010: Improving the Noah land surface model in arid regions with an appropriate parameterization of the thermal roughness length. *J. Hydrometeor.,* **11,** 995–1006.

——, ——, J. He, J. Qin, J. Shi, J. Du, and Q. He, 2011: Improving land surface temperature modeling for dry land of China. *J. Geophys. Res.,* **116,** D20104, doi:10.1029/2011jd015921.

Foken, T., and B. Wichura, 1996: Tools for quality assessment of surface-based flux measurements. *Agric. For. Meteor.,* **78,** 83–105.

Gockede, M., C. Rebmann, and T. Foken, 2004: A combination of quality assessment tools for eddy covariance measurements with footprint modelling for the characterisation of complex sites. *Agric. For. Meteor.,* **127,** 175–188.

Guo, X., and Coauthors, 2011: Critical evaluation of scalar roughness length parametrizations over a melting valley glacier. *Bound.-Layer Meteor.,* **139,** 307–332.

Helgason, W., and J. Pomeroy, 2011: Problems closing the energy balance over a homogeneous snow cover during midwinter. *J. Hydrometeor.,* **13,** 557–572.

Kanda, M., M. Kanega, T. Kawai, R. Moriwaki, and H. Sugawara, 2007: Roughness lengths for momentum and heat derived from outdoor urban scale models. *J. Appl. Meteor. Climatol.,* **46,** 1067–1079.

Lüers, J., and J. Bareiss, 2010: The effect of misleading surface temperature estimations on the sensible heat fluxes at a high Arctic site—The Arctic Turbulence Experiment 2006 on Svalbard (ARCTEX-2006). *Atmos. Chem. Phys.,* **10,** 157–168.

Ma, Y., Z. Su, T. Koike, T. Yao, H. Ishikawa, K. Ueno, and M. Menenti, 2003: On measuring and remote sensing surface energy partitioning over the Tibetan Plateau—From GAME/Tibet to CAMP/Tibet. *Phys. Chem. Earth,* **28,** 63–74.

——, S. Kang, L. Zhu, B. Xu, L. Tian, and T. Yao, 2008a: Tibetan Observation and Research Platform: Atmosphere–land interaction over a heterogeneous landscape. *Bull. Amer. Meteor. Soc.,* **89,** 1487–1492.

——, M. Menenti, R. Feddes, and J. Wang, 2008b: Analysis of the land surface heterogeneity and its impact on atmospheric variables and the aerodynamic and thermodynamic roughness lengths. *J. Geophys. Res.,* **113,** D08113, doi:10.1029/2007JD009124.

——, and Coauthors, 2009: Recent advances on the study of atmosphere–land interaction observations on the Tibetan Plateau. *Hydrol. Earth Syst. Sci.,* **13,** 1103–1111, doi:10.5194/hess-13-1103-2009.

——, L. Zhong, B. Wang, W. Ma, X. Chen, and M. Li, 2011: Determination of land surface heat fluxes over heterogeneous landscape of the Tibetan Plateau by using the MODIS and in situ data. *Atmos. Chem. Phys.,* **11,** 10 461–10 469.

Marks, D., A. Winstral, G. Flerchinger, M. Reba, J. Pomeroy, T. Link, and K. Elder, 2008: Comparing simulated and measured sensible and latent heat fluxes over snow under a pine canopy to improve an energy balance snowmelt model. *J. Hydrometeor.,* **9,** 1506–1522.

Massman, W. J., 1997: An analytical one-dimensional second-order closure model of turbulence statistics and the Lagrangian time scale within and above plant canopies of arbitrary structure. *Bound.-Layer Meteor.,* **83,** 407–421.

Mauder, M., and T. Foken, 2011: Documentation and instruction manual of the eddy covariance software package TK2. Universität Bayreuth Arbeitsgebnisse Nr. 46, 60 pp. [Available online at http://opus4.kobv.de/opus4-ubbayreuth/frontdoor/index/index/docId/681.]

McMillen, R., 1988: An eddy correlation technique with extended applicability to non-simple terrain. *Bound.-Layer Meteor.,* **43,** 231–245.

Moore, C. J., 1986: Frequency response corrections for eddy correlation systems. *Bound.-Layer Meteor.,* **37,** 17–35.

Oku, Y., H. Ishikawa, and Z. Su, 2007: Estimation of land surface heat fluxes over the Tibetan Plateau using GMS data. *J. Appl. Meteor. Climatol.,* **46,** 183–195.

Owen, P. R., and W. R. Thomson, 1963: Heat transfer across rough surfaces. *J. Fluid Mech.,* **15,** 321–334.

Sheppard, P. A., 1958: Transfer across the earth's surface and through the air above. *Quart. J. Roy. Meteor. Soc.,* **84,** 205–224.

Sobrino, J. A., J. C. Jiménez-Muñoz, and L. Paolini, 2004: Land surface temperature retrieval from LANDSAT TM 5. *Remote Sens. Environ.,* **90,** 434–440.

Su, H., M. F. McCabe, E. F. Wood, Z. Su, and J. H. Prueger, 2005: Modeling evapotranspiration during SMACEX: Comparing two approaches for local- and regional-scale prediction. *J. Hydrometeor.,* **6,** 910–922.

Su, Z., 2002: The Surface Energy Balance System (SEBS) for estimation of turbulent heat fluxes. *Hydrol. Earth Syst. Sci.,* **6,** 85–99.

——, T. Schmugge, W. P. Kustas, and W. J. Massman, 2001: An evaluation of two models for estimation of the roughness height for heat transfer between the land surface and the atmosphere. *J. Appl. Meteor.,* **40,** 1933–1951.

——, T. Zhang, Y. Ma, L. Jia, and J. Wen, 2006: Energy and water cycle over the Tibetan Plateau: Surface energy balance and turbulent heat fluxes. *Adv. Earth Sci.,* **21,** 1224–1236.

Tao, S.-Y., and Y.-H. Ding, 1981: Observational evidence of the influence of the Qinghai-Xizang (Tibet) Plateau on the occurrence of heavy rain and severe convective storms in China. *Bull. Amer. Meteor. Soc.,* **62,** 23–30.

Van der Kwast, J., and Coauthors, 2009: Evaluation of the Surface Energy Balance System (SEBS) applied to ASTER imagery with flux-measurements at the SPARC 2004 site (Barrax, Spain). *Hydrol. Earth Syst. Sci.,* **13,** 1337–1347.

Verhoef, W., M. Menenti, and S. Azzali, 1996: A colour composite of NOAA-AVHRR-NDVI based on time series analysis (1981–1992). *Int. J. Remote Sens.,* **17,** 231–235.

Vickers, D., and L. Mahrt, 1997: Quality control and flux sampling problems for tower and aircraft data. *J. Atmos. Oceanic Technol.,* **14,** 512–526.

Wang, S., and Y. Ma, 2011: Characteristics of land–atmosphere interaction parameters over the Tibetan Plateau. *J. Hydrometeor.,* **12,** 702–708.

——, Y. Zhang, S. Lü, H. Liu, and L. Shang, 2013: Estimation of turbulent fluxes using the flux-variance method over alpine meadows surface in eastern Tibetan Plateau. *Adv. Atmos. Sci.,* **30,** 411–424.

Wang, Y., X. Xu, A. R. Lupo, P. Li, and Z. Yin, 2011: The remote effect of the Tibetan Plateau on downstream flow in early summer. *J. Geophys. Res.,* **116,** D19108, doi:10.1029/2011jd015979.

Webb, E. K., G. I. Pearman, and R. Leuning, 1980: Correction of flux measurements for density effects due to heat and water vapour transfer. *Quart. J. Roy. Meteor. Soc.,* **106,** 85–100.

Wilczak, J., S. Oncley, and S. Stage, 2001: Sonic anemometer tilt correction algorithms. *Bound.-Layer Meteor.,* **99,** 127–150.

Yang, D., H. Chen, and H. Lei, 2010: Estimation of evapotranspiration using a remote sensing model over agricultural land in the North China Plain. *Int. J. Remote Sens.,* **31,** 3783–3798.

Yang, K., T. Koike, H. Fujii, K. Tamagawa, and N. Hirose, 2002: Improvement of surface flux parametrizations with a turbulence-related length. *Quart. J. Roy. Meteor. Soc.,* **128,** 2073–2087.

——, and Coauthors, 2008: Turbulent flux transfer over bare-soil surfaces: Characteristics and parameterization. *J. Appl. Meteor. Climatol.,* **47,** 276–290.

Zeng, X., and R. E. Dickinson, 1998: Effect of surface sublayer on surface skin temperature and fluxes. *J. Climate,* **11,** 537–550.

Zhang, X., 2010: Simulation of the bare soil surface energy balance at the Tongyu reference site in semiarid area of north China. *Atmos. Oceanic Sci. Lett.,* **3,** 330–335.

Zhou, D., R. Eigenmann, W. Babel, T. Foken, and Y. Ma, 2010: The study of near-ground free convection conditions at Nam Co station on the Tibetan Plateau. *Theor. Appl. Climatol.,* **105,** 1–12.